

RESEARCH ARTICLE

Stable and Tunable PT-Symmetric Single-Longitudinal-Mode Fiber Laser Using a Nonreciprocal Sagnac Loop

LIUYUAN TAO, FEI WANG^{ID}, ZHENGMAO WU^{ID}, AND GUANGQIONG XIA^{ID}School of Physical Science and Technology, Southwest University, Chongqing 400715, China
Institute of Electrical and Electronic Engineering, Chongqing University of Technology, Chongqing 400054, China

Corresponding author: Fei Wang (wangf17@swu.edu.cn)

This work was supported in part by the Fundamental Research Funds for the Central Universities of China under Grant SWU020001; and in part by the National Natural Science Foundation of China under Grant 61575034, Grant 61775184, Grant 61875167, and Grant 61875168.

ABSTRACT A stable and tunable parity-time (PT) symmetric single-longitudinal-mode fiber laser using a nonreciprocal Sagnac loop is proposed, which is experimentally and numerically demonstrated. The nonreciprocal Sagnac loop only including a 3-dB optical coupler (OC) and a polarization controller (PC) is incorporated into a fiber ring cavity, in which the nonreciprocal light transmission between frequency-degenerate clockwise (CW) and counterclockwise (CCW) resonator modes is induced to suppress multiple-longitudinal-mode oscillation of the laser. The two light paths along the CW and CCW directions in the Sagnac loop are respectively defined as the gain and loss loops of the PT-symmetric laser, due to a controllable birefringence induced by the PC. By controlling the polarization states of the two light waves, the PT symmetry is broken when the gain coefficient is larger than the coupling coefficient, single-mode lasing is thus achieved. Experimental results show that the optical signal to noise ratio (OSNR) of the single-mode lasing at 1550 nm is 43.0 dB, proving the great superiority of PT symmetry for lasing mode selection. By tuning an optical tunable band-pass filter incorporated into the fiber cavity, the wavelength of single-mode lasing varies from 1530 to 1560 nm, and their 3-dB Lorentzian linewidth varies within a range from 529 to 687 Hz. During a 30-min observation period, the variations of wavelength drift and OSNR of the single-mode lasing are less than 6 pm and 2.42 dB, respectively. The advantages of the proposed scheme are obvious, which include simple structure, low cost, simple operation, and good stability.

INDEX TERMS Fiber laser, single-longitudinal-mode, parity-time symmetry, nonreciprocal Sagnac loop.

I. INTRODUCTION

Single-longitudinal-mode fiber lasers possess inherent advantages of high beam quality, narrow linewidth, and low phase noise, demonstrating various promising applications, such as laser detection, fiber sensing, optical communication, and instrument testing. Up to now, for single-longitudinal-mode fiber laser, there are two main classifications in terms of form of laser cavity: linear cavity and ring cavity. For linear cavity, because spatial hole burning can be induced by standing wave effect [1], laser mode hopping is inevitable [2]. However, ring cavity can guarantee unidirectional circulation

of light waves to avoid spatial hole burning, which can alleviate mode hopping to some extent. In addition, according to the well-versed Schawlow-Townes formula [3], the ring laser with a longer cavity length has a longer photon lifetime, in which narrower linewidth is easier to obtain [4]. Therefore, numerous approaches have been proposed to achieve single-longitudinal-mode oscillation from fiber ring laser, such as employing a phase-shifted fiber Bragg grating (FBG) to form an ultra-narrow filter [5], utilizing an un-pumped Er^{3+} -doped fiber as a saturable absorber [6], adopting a compound-ring cavity structure based on Vernier effect [7], and the combination of two or even more of these schemes [8]. Nevertheless, for fiber ring laser, cavity length cannot be increased indefinitely. Over-long cavity length not only introduces

The associate editor coordinating the review of this manuscript and approving it for publication was Tianhua Xu^{ID}.

unnecessary loss, but also leads to closely spaced longitudinal modes, which is not conducive to achieve a single-mode operation.

In recent years, a new concept, parity-time (PT) symmetry [9], has been introduced and applied to the field of photonics for laser mode selection, which is a more efficient solution than the traditional method. PT symmetry, originating from quantum physics [10], was first proposed in 1998 by Bender and Boettcher [9]. To satisfy PT symmetry condition, the gain of one cavity should be of the same order of magnitude as the loss of the other cavity in two coupled microresonators [11], [12]. When PT symmetry is broken, the gain contrast expressed by the difference between the principal mode and the next competing mode of the system is greatly enhanced, thus making single-mode oscillation easier to implement. In 2014, Hodaei et al. first demonstrated that single-mode lasing can be readily achieved in a PT-symmetric microring laser [13]. In 2020, Yao et al. proposed a PT-symmetric laser formed by two mutually coupled optical fiber loops for mode selection [4]. However, in practice, the implementation is challenging to ensure the precise consistency of two optical loops, which greatly increases the difficulty of experimental operation. In view of this, to realize stable single-mode lasing, a PT-symmetric fiber ring laser with a single physical loop has been studied more widely in the field of optics [14], [15], [16], [17], [18], [19].

Herein, we propose and demonstrate a stable and tunable PT-symmetric single-longitudinal-mode fiber laser using a nonreciprocal Sagnac loop. An optical tunable filter (OTF) with a 3-dB bandwidth of 0.35 nm is used to coarsely select lasing mode, but there are still numerous closely spaced longitudinal modes under the narrow filter bandwidth. In order to obtain the stable single-mode operation, a Sagnac loop only including a 3-dB optical coupler (OC) and a polarization controller (PC) is constructed, in which the nonreciprocal light transmission along clockwise (CW) and counterclockwise (CCW) directions is induced. The CW and CCW birefringence paths introduced by the PC in opposite propagation directions are defined as the gain and loss loops of the PT-symmetric laser, respectively. The PT symmetry between the frequency-degenerate resonator modes along two different loops is broken only by adjusting a single PC, and single-mode lasing is such generated. Compared with the references [14], [15], a complicated Sagnac loop containing a polarization beam splitter (PBS) and two PCs is substituted by a simplified Sagnac loop only including a single PC, which simplifies system structure; more importantly, just by adjusting a PC, leading to nonreciprocal light transmission to meet the PT symmetry, which makes the system operation more convenient. In addition, in the reference [16], a Sagnac loop based on a microdisk resonator (MDR) and two PCs was used to generate a PT symmetric single-mode laser, by comparison, the fabrication process of device is complicated, and it is difficult to achieve coupling between the integrated device and optical fiber; furthermore, additional temperature control is required to tune lasing wavelength, which further increases

structural complexity and system cost. Therefore, the proposed configuration has prominent advantages in terms of system cost and practical operation.

The single-longitudinal-mode operation is successfully accomplished in the proposed PT-symmetric laser, the optical signal to noise ratio (OSNR) reaches 43.0 dB at 1550 nm, which proves the effectiveness of PT symmetry for mode selection. By changing the center wavelength of the OTF, the single-mode lasing wavelength can be tuned from 1530 to 1560 nm. The 3-dB linewidths of single-mode lasing under Lorentz fitting reach the sub-KHz level, with the minimum value of 529 Hz and the maximum value of 687 Hz over a span of 30 nm. It is worth noting that the single-mode operation of the proposed laser only relies on adjusting a single PC to break the PT symmetry, which not only simplifies system operation, but also benefits system stability. For the laser output in the single-mode state, the maximum lasing wavelength variation and OSNR fluctuation are respectively 6 pm and 2.42 dB during a 30-min test period for system stability.

II. PREPARATION EXPERIMENTAL SETUP AND OPERATION PRINCIPLE

A. EXPERIMENTAL SETUP

The proposed PT-symmetric fiber ring laser is depicted in Fig. 1(a). An 18-m commercial erbium-doped fiber (EDF) serves as an active fiber, which is core-pumped by a 980 nm light source providing a maximum output power of 700 mW via a wavelength division multiplexer (WDM). As such, a homemade erbium-doped fiber amplifier (EDFA) is formed to provide the gain of laser cavity. An OTF (Santec OTF-320-05S2) with a fix 3-dB bandwidth of 0.35 nm is implemented to determine lasing wavelength and select longitudinal modes preliminarily. A circulator (Cir) is employed to ensure that the light field circulates along one direction in the laser cavity to resist mode hopping induced by spatial hole burning and deliver the light wave into the Sagnac loop. The Sagnac loop only consists of a 3-dB OC (OC1) and a PC, forming two mutually coupled loops that transmit light waves in opposite directions. Thus, a PT-symmetric structure with the same geometric gain and loss loops is established. The PT symmetry condition is satisfied by the modal coupling between the CW (representing gain) and CCW (representing loss) travelling modes within the Sagnac loop. By adjusting the PC, a transition occurs from PT symmetry to PT symmetry breaking. The whole process requires neither additional optical gain nor additional loss injection, thus avoiding the associated noise caused by redundant components [20]. Finally, the light waves pass through the OC1 again and return to the laser cavity to form resonance. The lasing is extracted from the other end of the OC1 as output. In order to observe simultaneously, a 20:80 OC (OC2) divides the output lasing into two parts, 20% of which is directly captured by a high-precision optical spectrum analyzer (OSA, Aragon Photonics BOSA, 20 MHz resolution) for optical spectrum analysis, and

80% of which is used for lasing mode and linewidth analysis with the delayed self-heterodyne method. Fig. 1(b) presents the experimental setup of the delayed self-heterodyne method for laser linewidth test [21]. The light wave from the proposed laser is divided into two branches by a 3-dB OC (OC3). In the upper branch, the light wave is launched into a 40-km single mode fiber (SMF) as the delay line to break its coherence; in the lower branch, the light wave is transmitted into an acoustic optical modulator (AOM, G-1550-80) with an 80 MHz frequency shift, driven by a 24 V DC voltage supply, to keep it away from the carrier interference. The two signals are superimposed via another 3-dB OC (OC4) and then detected by a photodetector (PD, XPDV2120R, 50 GHz bandwidth). The output electrical signal is analyzed through an electrical spectrum analyzer (ESA, R&S FSW, 67 GHz bandwidth).

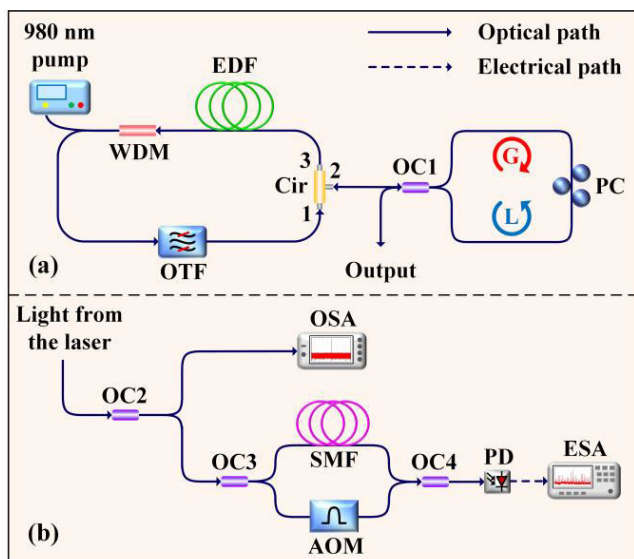


FIGURE 1. (a) Experimental setup of the proposed PT-symmetric fiber ring laser, (b) Experimental setup of the delayed self-heterodyne method for laser linewidth test. WDM: wavelength division multiplexer; EDF: erbium-doped fiber; Cir: circulator; OTF: optical tunable filter; OC: optical coupler; PC: polarization controller; SMF: single mode fiber; AOM: acoustic optical modulator; PD: photodetector; ESA: electrical spectrum analyzer; OSA: optical spectrum analyzer; G: gain; L: loss.

B. PT SYMMETRY

In general, non-Hermitian Hamiltonians tend to have complex eigenvalues [11]. However, Bender and Boettcher have shown that non-Hermitian Hamiltonians obeying a special form of PT symmetry own real eigenvalues [9]. Moreover, PT-symmetric Hamiltonians can undergo a phase transition, known as an exceptional point (EP) [22], which appears between PT symmetry and PT symmetry breaking. At such the EP, two eigenvalues and corresponding eigenvectors of PT-symmetric Hamiltonians simultaneously coalesce, resulting in their degeneracy [11]. Normally, a PT-symmetric system is established in two mutually coupled optical loops, in which one loop presents gain and the other loop presents

loss. By precisely controlling the gain, loss, and coupling coefficients, single-mode lasing can be satisfied well when the PT symmetry is broken.

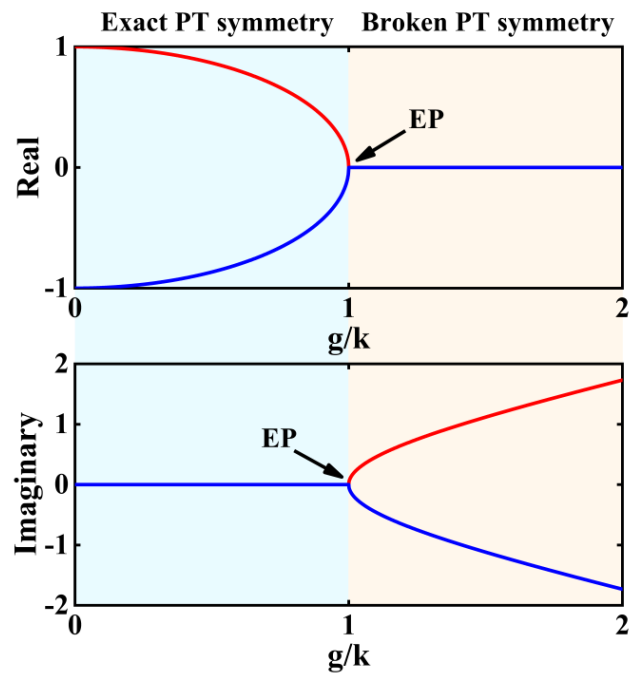


FIGURE 2. A schematic transition in the eigenfrequencies from exact PT symmetry to broken PT symmetry. EP: exceptional point.

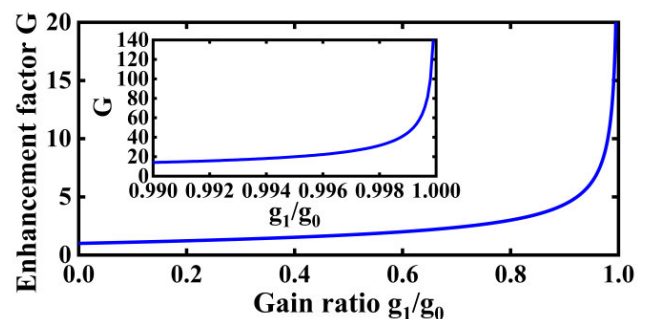


FIGURE 3. Enhancement factor as a function of gain ratio.

Within the context of coupled-mode theory [23], the equation governing the PT-symmetric system reads

$$\frac{d}{dt} \begin{pmatrix} a_1 \\ a_2 \end{pmatrix} = -i\hat{H} \begin{pmatrix} a_1 \\ a_2 \end{pmatrix}, \tag{1}$$

where a_1 and a_2 are the modal amplitudes in two coupled loops, and the effective Hamiltonian \hat{H} is given by [12] and [22]

$$\hat{H} = \begin{pmatrix} w_1 - ig & k \\ k & w_2 - il \end{pmatrix}, \tag{2}$$

where w_1 and w_2 take account of two eigenfrequencies without PT symmetry. g and l represent the gain and loss coefficients, respectively. And k denotes the coupling strength

between the two optical loops, which is mainly determined by the 3-dB OC1 [16]. Assuming the same delay in two coupled loops, we have $w_1 = w_2 = w$. By optimizing the system parameters, the PT symmetry condition is satisfied when $g = -l$, then the eigenfrequencies of this Hamiltonian are simplified to

$$w'_{\pm} = w \pm \sqrt{k^2 - g^2}. \quad (3)$$

Eq. (3) reveals that if the coupling strength is large enough ($k > g$), the system operates in the exact PT symmetry phase with real eigenfrequencies; for the weak coupling regime ($k < g$), the system becomes a pair of complex conjugate eigenfrequencies with the imaginary parts representing amplification and dissipation, illustrating the system locates in the broken PT phase. It is worth stressing that the transition point ($k = g$) is the so-called EP, as marked in Fig. 2. Since the evolution process of eigenfrequencies is mainly reflected in the second term of (3), in order to more clearly show the difference between the real part and imaginary part from PT symmetry to PT symmetry breaking, w in (3) is set as 0 in Fig. 2.

For a conventional laser, the gain contrast between the principal mode gain g_0 and the next competing mode gain g_1 is expressed by $g_{\max} = g_0 - g_1$. However, in a PT-symmetric laser, if the system is excited, the principal mode will first break PT symmetry and perform amplification, whereas the other modes undergo bounded oscillations [13]. Thus, a new definition of gain contrast is proposed for the PT-symmetric laser, which is rewritten as $g_{\max_PT} = \sqrt{g_0^2 - g_1^2}$ [12]. As a result, the laser with a PT-symmetric setting shows superior mode selection ability compared to that without PT-symmetric configuration. To further quantify the gain improvement caused by the square-root behavior, we calculate the enhancement factor G , given by

$$G = \frac{g_{\max_PT}}{g_{\max}} = \sqrt{\frac{g_0/g_1 + 1}{g_0/g_1 - 1}}. \quad (4)$$

The simulation results of (4) are shown in Fig. 3. A sharply increasing is appeared, especially as g_1 approaches g_0 , demonstrating the effective mode selection capability of PT symmetry.

C. NONRECIPROCAL LIGHT TRANSMISSION

Nonreciprocal light transmission in the Sagnac loop is described in Fig. 4. E_{IN} represents the electric field of input light beam entering the Sagnac loop, which is then divided by the OC1 into two light beams traveling in opposite directions, denoted by E_{CW} and E_{CCW} respectively. After passing through the PC, the two light waves are represented as E'_{CW} and E'_{CCW} , and finally combine at OC1 and output from the Sagnac loop. The electric field at the reflection and transmission ports of the Sagnac loop are expressed as E_R and E_T , respectively. The presence of PC is equivalent to the introduction of a controllable birefringence into the Sagnac loop. For

E_{CW} and E_{CCW} , although the intensity of PC birefringence effect is the same, the angle (denoted by Ω) between the polarization direction and the fast axis orientation of PC birefringence effect is different due to the opposite direction of E_{CW} and E_{CCW} entering the PC, thus enabling the phase delay (denoted by 2δ) of E_{CW} and E_{CCW} after transmission by the PC to be different. Therefore, Ω and 2δ jointly characterize the transmission matrix of PC, resulting in a different phase delay between E'_{CW} and E'_{CCW} . In this way, the reflectance of the Sagnac loop is determined by both the beam ratio of OC1 and the birefringence induced by PC. Although the beam ratio of OC1 is fixed, the fast axis orientation and intensity of birefringence can be changed by adjusting the state of PC, thus changing the reflectance of the Sagnac loop [17], [24]. Subsequently, the necessary asymmetry is established between two light waves propagating in opposite directions within the Sagnac loop, and the nonreciprocal light transmission between the frequency-degenerate CW and CCW resonator modes is formed. As adjusting the PC, the asymmetry is further amplified, leading to the appearance of gain and loss loops, which is numerically expressed as gain and loss coefficients. Here, we assume that the light wave propagating along the CW direction is the gain loop, and the CCW one is the loss loop. When the light waves circulate several times in the resonant cavity, the nonreciprocal effect is enhanced. To implement PT symmetry, the polarization phase retardances of two light waves is eliminated by adjusting two quarter-wave plates of PC, which ensures the consistency of the real parts of eigenfrequencies in the resonator cavity. Then, once the gain coefficient is greater than the coupling coefficient for one mode, stable single-mode lasing with PT broken can be achieved, which is called the principal mode, or the 0th-mode.

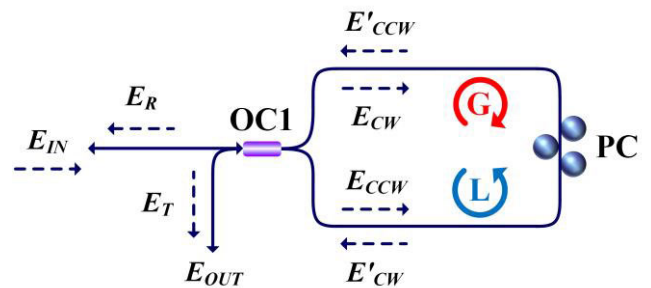


FIGURE 4. Nonreciprocal light transmission in the Sagnac loop.

Since the reflection and transmission of the Sagnac loop are results of the interference coupling of nonreciprocal light transmission, and the reflected and transmitted energies are complementary, the nonreciprocal degree of light fields can be estimated simply by the reflected to transmitted light power ratio of the Sagnac loop. In order to explore the greatest nonreciprocal effect, the PC is adjusted to maximize the power difference between the reflected and transmitted signals, when a continuous light located at 1547.82 nm is injected into the Sagnac loop. The normalized optical spectra

are shown in Fig. 5, where the reflection and transmission spectrum are indicated by lines in red and blue respectively. The results reveal that the normalized intensity of reflected and transmitted signals is 0.8470 and 0.0034 respectively, which fully proves the excellent nonreciprocal property of the Sagnac loop. The inset in Fig. 5 is the optical spectra directly measured by OSA with the maximum isolation ratio of 23.96 dB. By manually adjusting the three wave plates of PC, the isolation ratio can be varied arbitrarily from zero to the maximum value, which indirectly reflects the variation of gain and loss coefficients. The nonreciprocal property of the Sagnac loop can be fully achieved only by controlling one PC. As long as the appropriate polarization states of two light waves are determined, the gain and loss loops are naturally established, and the PT symmetry of 0th-mode is broken when the gain coefficient is greater than the coupling coefficient. However, the rest of higher-order modes retain PT unbroken due to their stronger coupling coefficients than the 0th-mode [25]. In fact, despite the variation in the polarization state of light waves, the 0th-mode always has a coordinate system corresponding to the PT symmetry breaking, while the other modes are completely confined to the PT unbroken regime [26]. Thus, a stable single-mode lasing based on the nonreciprocal light transmission is realized.

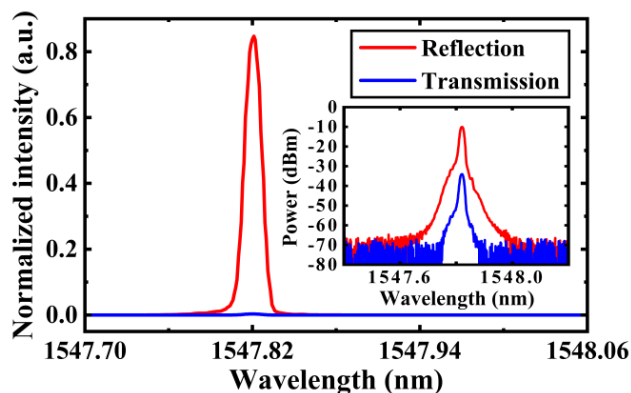


FIGURE 5. Normalized reflection and transmission spectra of the Sagnac loop with the maximum power difference, where insert is optical spectra directly measured by OSA.

III. RESULTS AND DISCUSSION

The optical spectral response of OTF is shown by the blue line in Fig. 6. The 3-dB bandwidth of OTF is 0.35 nm. The cavity length of the proposed PT-symmetric laser is about 32.3 m, and the corresponding longitudinal mode interval is 6.19 MHz. Without PT symmetry, the multimode oscillation occurs in the laser cavity with more than 7000 longitudinal modes at 0.35 nm bandwidth. To simulate the PT symmetry condition, each mode in the filter bandwidth is multiplied by the corresponding enhancement factor in (4) to achieve the mode self-competition. From Fig. 3, as the next competing mode gain extremely approaches the principal mode gain, the enhancement factor increases dramatically, which

in turn inhibits the gain of side modes, resulting in a huge gain difference with the principal mode. The calculated gain curve, shown by the red line in Fig. 6, can be equivalent to an ultra-narrow bandwidth filtering function, in which only one mode can continue to oscillate whereas the other modes are strongly suppressed. The effectiveness of mode selection for PT symmetry is fully manifested with the enhancement factor. The inset in Fig. 6 plots the detailed optical spectra without (blue) and with (red) PT symmetry in black dashed box. The gain contrast between the principal mode and the next competing mode is enhanced by 27.15 dB, which is sufficient for the system to make the single-mode oscillation possible with the adoption of PT symmetry.

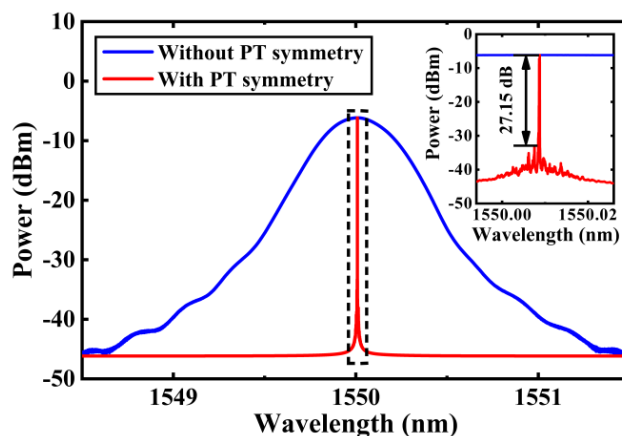


FIGURE 6. Measured optical spectral response (blue) of OTF at 1550 nm and simulated equivalent filtering curve (red) under PT symmetry condition, where insert is detailed optical spectra in black dashed box.

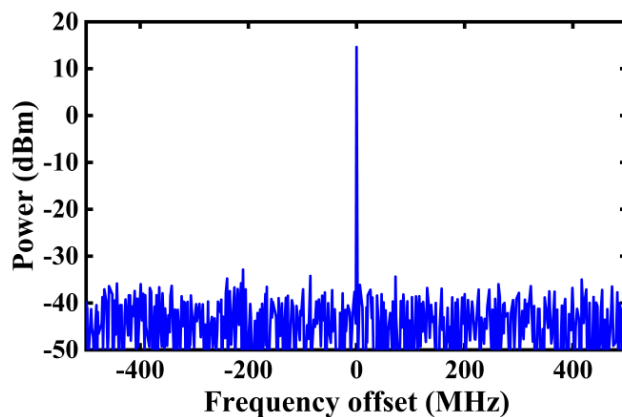


FIGURE 7. Simulated electrical spectrum of single-mode oscillation with PT symmetry breaking.

Firstly, the proposed PT-symmetric laser is simulated to verify the above analysis using the theoretical model in [24]. The use of PC within the Sagnac loop provides dual control over the intensity and phase of light waves transmitted in opposite directions [27], which can be modulated in the simulation by assigning different values to the azimuth and

ellipticity of the PC. Until the PT symmetry of the principal mode is broken, presenting a large gain difference with side modes, a stable single-mode lasing is produced, as shown in Fig. 7. The results manifest that in the frequency range of 1 GHz, only the principal mode with a dominant intensity is retained, which theoretically demonstrates the ability of PT symmetry for suppressing multimode oscillation.

Fig. 8 shows that the output spectrum of the proposed PT-symmetric laser measured by the high-precision OSA. The wavelength of output lasing is 1550 nm, and the OSNR is 43.0 dB without any parasitic lasing in the wavelength range of 10 nm. Compared with the references [15], [16], the suppression ability of side modes is slightly improved in the proposed scheme. In the inset of Fig. 8, the optical spectrum range has been further reduced to 0.02 nm, however, due to the resolution limit of OSA, we still cannot confirm that the obtained lasing stably oscillates in the single-mode state.

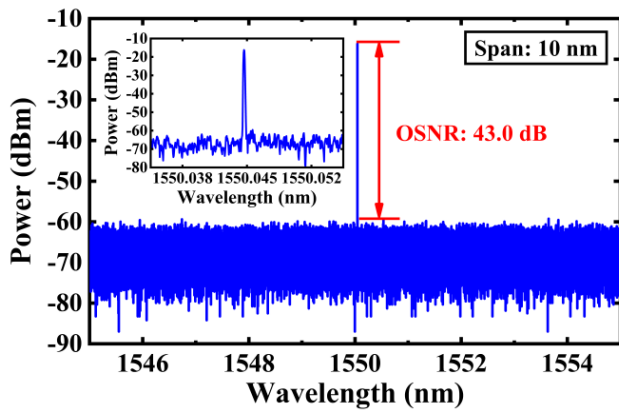


FIGURE 8. Measured optical spectrum of the PT symmetric laser at 1550 nm.

To further confirm that the laser output is single-mode state, the delayed self-heterodyne method is utilized. The measurement is conducted in the situation without and with PT symmetry breaking, and the related results are plotted in Figs. 9(a)-(d), respectively. Fig. 9(a) shows the multimode oscillation in a span of 160 MHz. In this situation, PT symmetry breaking is not enabled. Then, we alter the spectrum scanning range to 20 MHz. It can be seen from Fig. 9(b) that the longitudinal mode interval is 6.19 MHz, which corresponds to a 32.3 m fiber loop length. To achieve single-mode oscillation, we adjust the PC to reach the PT symmetry breaking condition. The recorded RF spectra are notably different from the previous situation. It is apparent that only a dominating mode is successfully retained whereas the side modes are greatly suppressed in a span of 160 MHz in Fig. 9(c) and 20 MHz in Fig. 9(d). The above analysis indicates that the proposed laser can guarantee the single-mode output state.

For comparison, we remove the Sagnac loop and only use the OTF with a 0.35-nm bandwidth, the output characteristic of the laser is measured again by ESA. From Fig. 10, a large number of densely spaced longitudinal modes are produced

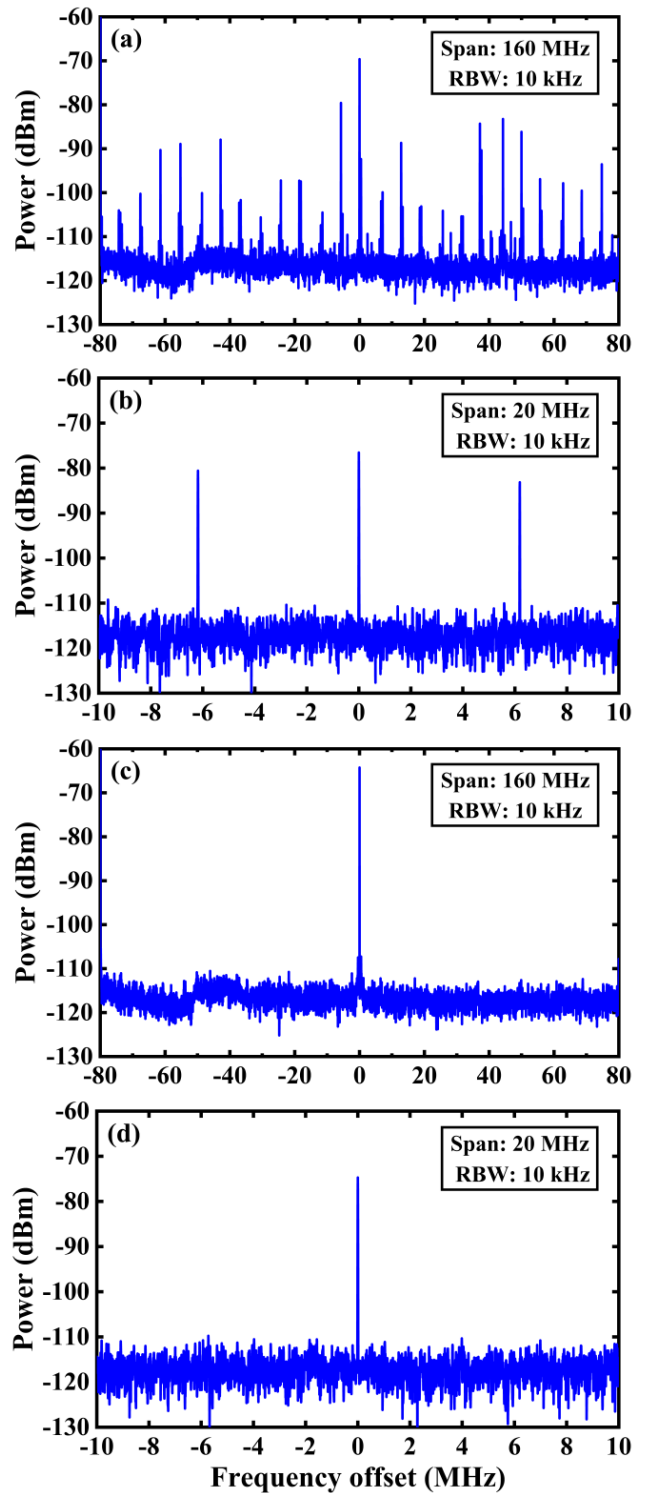


FIGURE 9. Measured electrical spectra of the proposed laser at 1550 nm for multimode oscillation without PT symmetry breaking in a span of 160 MHz (a) and 20 MHz (b), and single-mode oscillation with PT symmetry breaking in a span of 160 MHz (c) and 20 MHz (d).

in the OTF bandwidth, and the modes compete fiercely with each other. This fully demonstrates the critical role of the Sagnac loop.

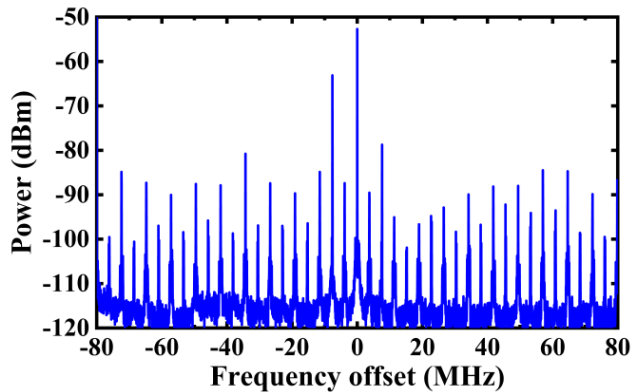


FIGURE 10. Measured electrical spectra of the proposed laser without the Sagnac loop.

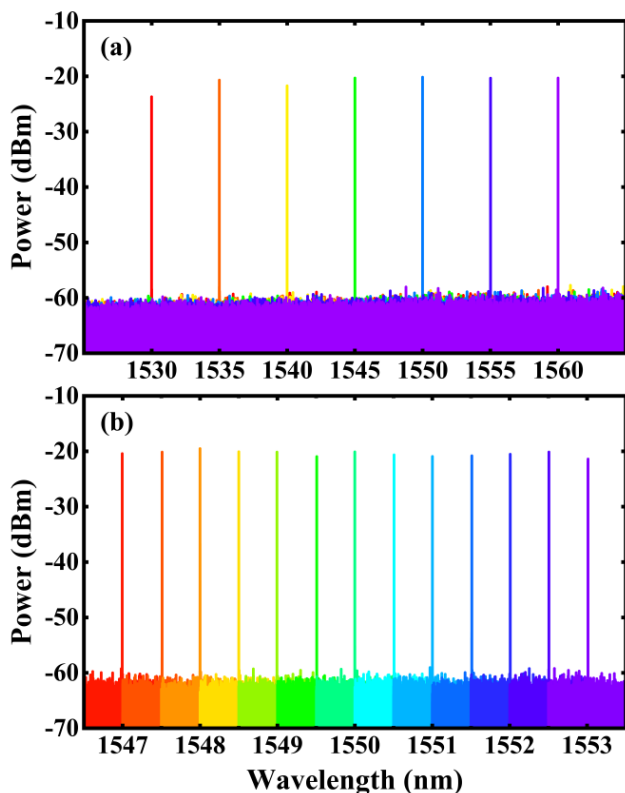


FIGURE 11. Optical spectra of the proposed laser at wavelengths (a) from 1530 to 1560 nm with a step of 5 nm and (b) from 1547 to 1553 nm with a step of 0.5 nm.

Then, by tuning the OTF, the available wavelength range of the proposed PT-symmetric laser is studied. The single-mode lasing is maintained during the wavelength tuning process. Fig. 11(a) shows the effective lasing wavelength of the proposed laser spans 30 nm from 1530 to 1560 nm. To prove the continuous wavelength tunability, the optical spectrum of output lasing is fine-tuned from 1547 to 1553 nm with a step of 0.5 nm, as displayed in Fig. 11(b). The available wavelength range can be further enlarged by optimizing the

length of EDF [28]. However, in the references [16] and [19], the wavelength tunable range of 1.194 nm and 0.16 nm is extremely limited, which fully reflects the advantage of proposed scheme in wavelength by comparison.

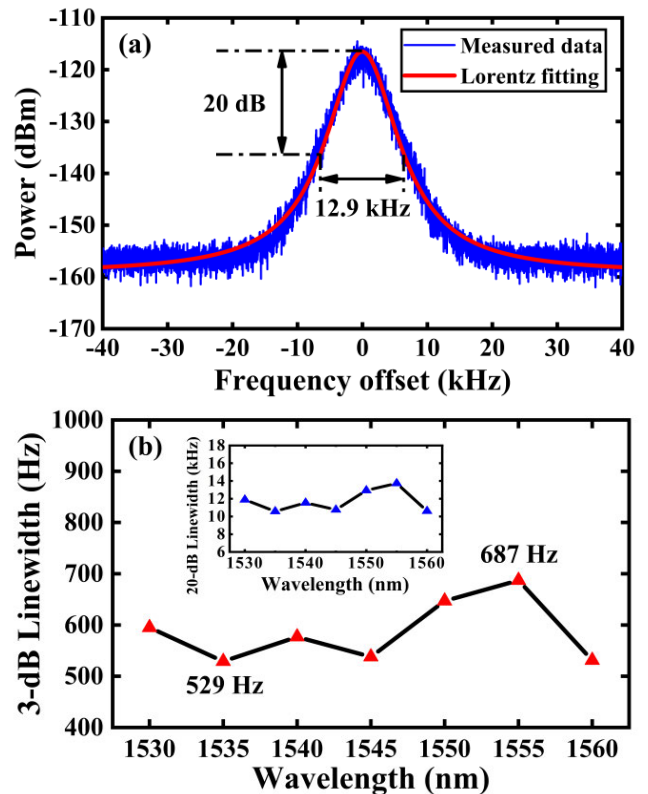


FIGURE 12. (a) RF signal measured by the delayed self-heterodyne method and Lorentz fitting curve at 1550 nm and (b) Variation of 3-dB linewidth at different wavelengths, where insert is 20-dB linewidth value.

Moreover, we investigate the linewidth characteristics of output lasing on the premise of single-mode operation. The output electrical spectra and Lorentz fitting curve at 1550 nm are presented in Fig. 12(a). Considering the inevitable $1/f$ frequency noise caused by the long delayed fiber [29], the 3-dB spectral width derived from the 20-dB spectral width is more accurate than the 3-dB spectral width measured directly for the Lorentz fitting curve. The 20-dB linewidth of the RF signal obtained at 1550 nm is 12.9 kHz, and the corresponding 3-dB linewidth is 645 Hz. To observe the influence of the laser wavelength variation on the lasing linewidth, we take the same method to measure the linewidth several times from 1530 to 1560 nm at a 5-nm wavelength interval. Fig. 12(b) plots the variation of the calculated 3-dB linewidth value over the available wavelength range according to the Lorentz fitting curve, where the inset is the corresponding 20-dB linewidth value. All the 3-dB linewidths of the proposed laser are less than 687 Hz when the laser wavelength varies within 30 nm, and the 3-dB linewidth with the minimum value of 529 Hz is obtained at 1535 nm. The variation of linewidth at different wavelengths may be caused by the poor gain flatness of the homemade EDFA, as well as the

influence of ambient noise, resulting from the system being placed in an open environment. However, it is worth noting that theoretically, the SMF length of 40 km is not sufficient to eliminate the influences of interference between two branches shown in Fig. 1(b). Thus, the measured linewidth should be regarded as a conservative estimation relative to the actual linewidth. Compared with the references [15] and [16], our experimental setup can also reduce the lasing linewidth to the sub-kHz level. In fact, the limit factors for the laser linewidth include laser gain, cavity length and output power [30].

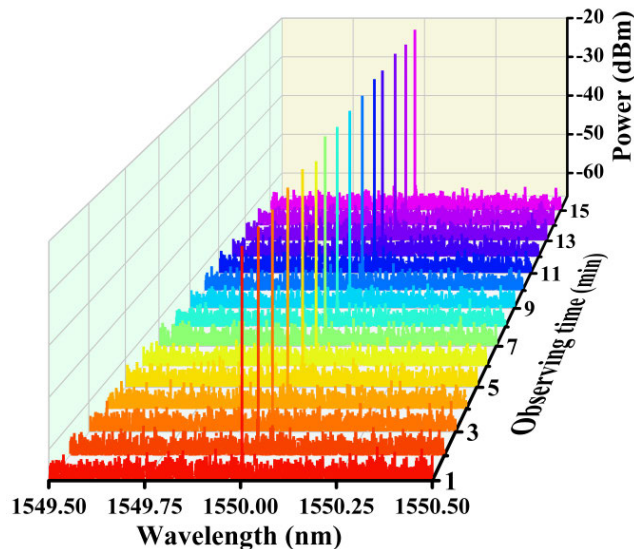


FIGURE 13. Optical spectrum of the lasing at 1550 nm in a 1-min interval over 15 min.

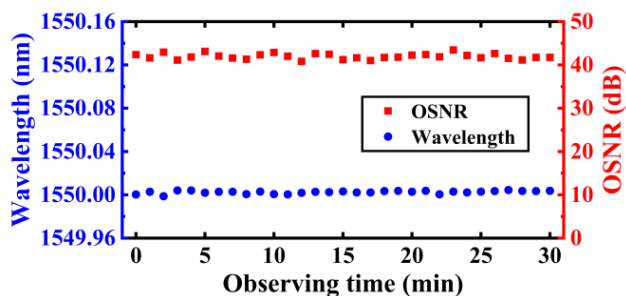


FIGURE 14. Fluctuations of the lasing wavelength and OSNR in a 1-min interval over 30 min.

To research the stability of the proposed PT-symmetric laser, we take the lasing wavelength operating at 1550 nm as a typical illustration to observe the output characteristics. As can be seen in Fig. 13, the stable single-mode lasing without significant variation is observed from the measured optical spectra with 15 times repeated scans at 1-min interval. At the same time, in the monitoring of the electrical spectra, the single-mode lasing operates stably at the 80 MHz frequency without other side modes. From the point of view of PT symmetry, as long as the polarization state is determined,

the principal mode satisfying the PT symmetry breaking condition remains oscillating in the current coordinate system, whereas the other modes remain suppressed. To further analyze the stability behavior, the fluctuations of the lasing wavelength and OSNR are recorded for 30-min with an interval of 1-min, as exhibited in Fig. 14. The diagram shows that the maximum variations of the single-mode lasing wavelength and OSNR are 6 pm and 2.42 dB, respectively. These slight changes may be attributed to the power instability caused by the 980 nm pump source, and the disturbance of cavity length induced by the external environment, such as temperature, mechanical vibration and so on.

IV. CONCLUSION

In summary, we have proposed and experimentally and numerically investigated a stable and tunable single-longitudinal-mode fiber ring laser based on PT symmetry, which is established by employing a simplified Sagnac loop only consisting of an OC and a PC. There are two light paths along the CW and CCW directions in the Sagnac loop, which are defined as the gain loop and loss loop of the PT-symmetric structure, respectively. Then, the nonreciprocal light transmission between the frequency-degenerate CW and CCW resonator modes is achieved by adjusting the PC in the Sagnac loop. Once the gain coefficient exceeds the coupling coefficient, the stable single-longitudinal-mode lasing is achieved without employing additional optical components. The OSNR of the single-mode lasing reaches 43.0 dB at 1550 nm, and only a dominating mode is obtained whereas the side modes are greatly suppressed in the RF spectra, which proves effective mode selection ability of PT symmetry. The lasing wavelength covering from 1530 to 1560 nm is achieved by tuning the OTF merged into the fiber ring laser. Over the wavelength tuning range of 30 nm, the Lorentz-fitted linewidth of single-mode lasing varies from 529 to 687 Hz. Furthermore, during a 30-min stability test of single-mode operation, the recorded fluctuations of lasing wavelength and OSNR are respectively less than 6 pm and 2.42 dB. We believe that the proposed PT-symmetric laser has potential applications for optical communication, microwave photonics and laser radar.

REFERENCES

- [1] J. J. Zayhowski, "Limits imposed by spatial hole burning on the single-mode operation of standing-wave laser cavities," *Opt. Lett.*, vol. 15, no. 8, pp. 431–433, Apr. 1990.
- [2] J. Ji, H. Wang, J. Ma, J. Guo, J. Zhang, D. Tang, and D. Shen, "Narrow linewidth self-injection locked fiber laser based on a crystalline resonator in add-drop configuration," *Opt. Lett.*, vol. 47, no. 6, pp. 1525–1528, Mar. 2022.
- [3] A. L. Schawlow and C. H. Townes, "Infrared and optical masers," *Phys. Rev.*, vol. 112, no. 16, pp. 1940–1949, 1958.
- [4] Z. Fan, W. Zhang, Q. Qiu, and J. Yao, "Observation of PT-symmetry in a fiber ring laser," *Opt. Lett.*, vol. 45, no. 4, pp. 1027–1030, Feb. 2020.
- [5] Y. Yao, X. Chen, Y. Dai, and S. Xie, "Dual-wavelength erbium-doped fiber laser with a simple linear cavity and its application in microwave generation," *IEEE Photon. Technol. Lett.*, vol. 18, no. 1, pp. 187–189, Jan. 1, 2006.

- [6] L. Huang, C. Yang, T. Tan, W. Lin, Z. Zhang, K. Zhou, Q. Zhao, X. Teng, S. Xu, and Z. Yang, "Sub-kHz-linewidth wavelength-tunable single-frequency ring-cavity fiber laser for C- and L-band operation," *J. Lightw. Technol.*, vol. 39, no. 14, pp. 4794–4799, Jul. 1, 2021.
- [7] C.-H. Yeh, W.-Y. You, J.-R. Chen, W.-P. Lin, C.-W. Chow, and J.-H. Chen, "A single-mode erbium fiber laser with flat power output and wide wavelength tunability," *IEEE Photon. J.*, vol. 12, no. 6, Dec. 2020, Art. no. 7202805.
- [8] Z. Wang, J. Shang, K. Mu, S. Yu, and Y. Qiao, "Stable single-longitudinal-mode fiber laser with ultra-narrow linewidth based on convex-shaped fiber ring and Sagnac loop," *IEEE Access*, vol. 7, pp. 166398–166403, 2019.
- [9] C. M. Bender and S. Boettcher, "Real spectra in non-Hermitian Hamiltonians having PT symmetry," *Phys. Rev. Lett.*, vol. 80, no. 24, pp. 5243–5246, Jun. 1998.
- [10] R. El-Ganainy, K. G. Makris, M. Khajavikhan, Z. H. Musslimani, S. Rotter, and D. N. Christodoulides, "Non-Hermitian physics and PT symmetry," *Nature Phys.*, vol. 14, no. 1, pp. 11–19, Jan. 2018.
- [11] A. Krasnok, N. Nefedkin, and A. Alu, "Parity-time symmetry and exceptional points [electromagnetic perspectives]," *IEEE Antennas Propag. Mag.*, vol. 63, no. 6, pp. 110–121, Dec. 2021.
- [12] K. Ozdemir, S. Rotter, F. Nori, and L. Yang, "Parity-time symmetry and exceptional points in photonics," *Nat. Mater.*, vol. 18, no. 8, pp. 783–798, Aug. 2019.
- [13] H. Hodaie, M. A. Miri, M. Heinrich, D. N. Christodoulides, and M. Khajavikhan, "Parity-time-symmetric microring lasers," *Science*, vol. 346, no. 6212, pp. 975–978, 2014.
- [14] Z. Dai, Z. Fan, P. Li, and J. Yao, "Frequency-tunable parity-time-symmetric optoelectronic oscillator using a polarization-dependent Sagnac loop," *J. Lightw. Technol.*, vol. 38, no. 19, pp. 5327–5332, Oct. 1, 2020.
- [15] Z. Dai, Z. Fan, P. Li, and J. Yao, "Widely wavelength-tunable parity-time symmetric single-longitudinal-mode fiber ring laser with a single physical loop," *J. Lightw. Technol.*, vol. 39, no. 7, pp. 2151–2157, Apr. 1, 2021.
- [16] Z. Fan, Z. Dai, Q. Qiu, and J. Yao, "Parity-time symmetry in a single-loop photonic system," *J. Lightw. Technol.*, vol. 38, no. 15, pp. 3866–3873, Aug. 1, 2020.
- [17] L. Li, Y. Cao, Y. Zhi, J. Zhang, Y. Zou, X. Feng, B.-O. Guan, and J. Yao, "Polarimetric parity-time symmetry in a photonic system," *Light, Sci. Appl.*, vol. 9, no. 1, p. 169, Sep. 2020.
- [18] Y. Wei, H. Zhou, D. Huang, F. Li, J. Dong, X. Zhang, and P. K. A. Wai, "Suppression and revival of single-cavity lasing induced by polarization-dependent loss," *Opt. Lett.*, vol. 46, no. 13, pp. 3151–3154, Jul. 2021.
- [19] Z. Deng, L. Li, J. Zhang, and J. Yao, "Single-mode narrow-linewidth fiber ring laser with SBS-assisted parity-time symmetry for mode selection," *Opt. Exp.*, vol. 30, no. 12, pp. 20809–20819, Jun. 2022.
- [20] S. Soleymani, Q. Zhong, M. Mokim, S. Rotter, R. El-Ganainy, and S. K. Özdemir, "Chiral and degenerate perfect absorption on exceptional surfaces," *Nature Commun.*, vol. 13, no. 1, p. 599, Feb. 2022.
- [21] T. Okoshi, K. Kikuchi, and A. Nakayama, "Novel method for high resolution measurement of laser output spectrum," *Electron. Lett.*, vol. 16, no. 16, pp. 630–631, Jul. 1980.
- [22] M.-A. Miri and A. Alu, "Exceptional points in optics and photonics," *Science*, vol. 363, no. 6422, Jan. 2019, Art. no. eaar7709.
- [23] H. Haus and W. P. Huang, "Coupled-mode theory," *Proc. IEEE*, vol. 79, no. 10, pp. 1505–1518, Oct. 1991.
- [24] Q. Qin, F. Yan, Y. Liu, Y. Guo, L. Zhang, B. Guan, T. Li, Y. Suo, H. Zhou, and T. Feng, "Multi-wavelength thulium-doped fiber laser via a polarization-maintaining Sagnac loop mirror with a theta-shaped configuration," *J. Lightw. Technol.*, vol. 39, no. 13, pp. 4517–4524, Jul. 2021.
- [25] M. Khajavikhan, H. Hodaie, M. A. Miri, and D. Christodoulides, "Single-mode parity-time-symmetric micro-ring lasers," in *Proc. IEEE CLEO-PR*, Busan, South Korea, 2015, Paper 28D2_1.
- [26] Y. Liu, T. Hao, W. Li, J. Capmany, N. Zhu, and M. Li, "Observation of parity-time symmetry in microwave photonics," *Light, Sci. Appl.*, vol. 7, no. 1, p. 38, Jul. 2018.
- [27] N. J. Muga, A. N. Pinto, M. F. S. Ferreira, and J. R. F. Da Rocha, "Uniform polarization scattering with fiber-coil-based polarization controllers," *J. Lightw. Technol.*, vol. 24, no. 11, pp. 3932–3943, Nov. 2006.
- [28] S. Yamashita, "Widely tunable erbium-doped fiber ring laser covering both C-band and L-band," *IEEE J. Sel. Topics Quantum Electron.*, vol. 7, no. 1, pp. 41–43, Jan. 2001.
- [29] L. B. Mercer, "1/f frequency noise effects on self-heterodyne linewidth measurements," *J. Lightw. Technol.*, vol. 9, no. 4, pp. 485–493, Apr. 1991.
- [30] M. Pollnau and M. Eichhorn, "Spectral coherence, Part I: Passive-resonator linewidth, fundamental laser linewidth, and schawlow-townes approximation," *Prog. Quantum Electron.*, vol. 72, Aug. 2020, Art. no. 100255.

LIUYUAN TAO received the B.S. degree from the College of Information Science and Engineering, Henan University of Technology, Zhengzhou, China, in 2019. She is currently pursuing the master's degree in signal and information processing with Southwest University, Chongqing, China. Her current research interest includes fiber laser.

FEI WANG received the Ph.D. degree in electronic science and technology from the Huazhong University of Science and Technology, Wuhan, China, in 2010. He is currently a Professor with the School of Physical Science and Technology, Southwest University, Chongqing, China. He is the author or coauthor of more than 120 journal articles and conference papers. His current research interests include all-optical signal processing, microwave photonics, fiber laser, and chaotic semiconductor lasers and their applications.

ZHENGMAO WU received the B.Sc., M.Sc., and Ph.D. degrees in optics from Sichuan University, Chengdu, Sichuan, China, in 1992, 1995, and 2003, respectively. He is currently a Professor with the School of Physical Science and Technology, Southwest University, Chongqing, China. He has authored or coauthored more than 200 journal articles and conference papers. His current research interests include nonlinear dynamics of semiconductor lasers and their applications, and microwave photonics.

GUANGQIONG XIA received the B.Sc., M.Sc., and Ph.D. degrees in optics from Sichuan University, Chengdu, Sichuan, China, in 1992, 1995, and 2002, respectively. She is currently a Professor with the School of Physical Science and Technology, Southwest University, Chongqing, China. She has authored or coauthored more than 200 publications. Her current research interest includes the nonlinear dynamics of semiconductor lasers and their applications.

• • •